

Rm-2675-P-3

RADC-TR-70-93  
Technical Report  
April 1970



1

Prepared By  
Rome Air Development Center  
Air Force Systems Command  
Griffiss Air Force Base, New York 13440

AD 739192

# PROJECT SECEDE

## STUDIES OF BARIUM EXCITATION BY MOLECULAR BEAM MAGNETIC RESONANCE TECHNIQUES

DDC  
REPRODUCED  
MAR 24 1972  
C

SPONSORED BY  
ADVANCED RESEARCH PROJECTS AGENCY  
ARPA ORDER NO. 1228.

PRINCIPAL INVESTIGATOR: ROBERT A. FLUEGGE  
PHONE: 716-832-7800 EXT 768

CONTRACT ENGINEER: JOSEPH J. SIMONS  
PHONE: 315 330-3451

PROJECT ENGINEER: VINCENT J. COYNE  
PHONE: 315 330-3107

Approved for public release;  
distribution unlimited.

NAME OF CONTRACTOR: CORNELL AERONAUTICAL  
LABORATORY  
CONTRACT NUMBER: F30502-59-C-0032  
EFFECTIVE DATE OF CONTRACT: 10 JULY 1959  
CONTRACT EXPIRATION DATE: 10 AUGUST 1970  
AMOUNT OF CONTRACT: \$84,850  
PROGRAM CODE NUMBER: 9E20

THE VIEWS AND CONCLUSIONS CONTAINED IN THIS DOCUMENT ARE THOSE  
OF THE AUTHORS AND SHOULD NOT BE INTERPRETED AS NECESSARILY  
REPRESENTING THE OFFICIAL POLICIES, EITHER EXPRESSED OR IMPLIED,  
OF THE ADVANCED RESEARCH PROJECTS AGENCY OR THE U. S. GOVERNMENT.

Reproduced by  
NATIONAL TECHNICAL  
INFORMATION SERVICE  
Springfield, Va 22151

33

# DISCLAIMER NOTICE

THIS DOCUMENT IS THE BEST  
QUALITY AVAILABLE.

COPY FURNISHED CONTAINED  
A SIGNIFICANT NUMBER OF  
PAGES WHICH DO NOT  
REPRODUCE LEGIBLY.

**UNCLASSIFIED**

Security Classification

**DOCUMENT CONTROL DATA - R & D**

*Security classification of title, body of abstract and indexing annotation must be entered when the overall report is classified*

1. ORIGINATING ACTIVITY (Corporate author) <b>Cornell Aeronautical Laboratory, Inc. Buffalo, New York 14221</b>		2a. REPORT SECURITY CLASSIFICATION <b>UNCLASSIFIED</b>	
		2b. GROUP	
3. REPORT TITLE <b>Studies of Barium Excitation by Molecular Beam Magnetic Resonance Techniques</b>			
4. DESCRIPTIVE NOTES (Type of report and inclusive dates) <b>Semi-Annual</b>			
5. AUTHOR(S) (First name, middle initial, last name) <b>Robert A. Fluegge Dr. Dale Headrick Dr. Donald Landman</b>			
6. REPORT DATE <b>April 1970</b>	7a. TOTAL NO. OF PAGES <b>27</b>	7b. NO. OF REFS <b>7</b>	
8a. CONTRACT OR GRANT NO. <b>F30602-69-C-0032</b>	9a. ORIGINATOR'S REPORT NUMBER(S)		
b. PROJECT NO. <b>1225</b>			
c.	9b. OTHER REPORT NUMBER(S) (Any other numbers that may be assigned this report)		
d.	<b>RADC-TR-70-93</b>		
10. DISTRIBUTION STATEMENT <b>Approved for public release; distribution unlimited.</b>			
11. SUPPLEMENTARY NOTES <b>Monitored by:</b> <b>Joseph J. Simons RADC (EMASA) GAFB, NY 13440 AC-315-330-3451</b>		12. SPONSORING MILITARY ACTIVITY <b>Advanced Research Project Agency Washington, D. C. 20301</b>	
13. ABSTRACT <p>This report presents the results of an investigation of Barium excitation by Molecular Beam Magnetic Resonance Techniques. The results of both depopulation and ionization experiments are consistent and confirm that the metastable states in barium are strong contributors to photoionization in barium clouds under solar radiation. The depopulation experiments indicate that the major losses occur due to photons near 3005 Å and that considerable metastable density increases occur when the atomic barium beam is subjected to a full light spectrum. The ionization experiments show that roughly half of the photo-ionization (for equally populated metastables) occurs from the singlets and half from the triplet metastable states. The Laboratory experiments indicate that ionization occurs mainly from photons having wavelengths longer than 3000 Å.</p> <p>The report also presents a discussion of the mechanisms that decrease metal atom densities with emphasis on barium oxide, aluminum oxide and boron oxide reactions.</p>			

KEY WORDS

LINK A

LINK B

LINK C

ROLE

WT

ROLE

WT

ROLE

WT

Barium Releases

Ionization Processes

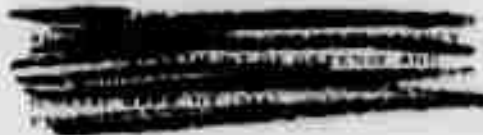
Metal Atom Loss Processes

**STUDIES OF BARIUM EXCITATION BY MOLECULAR  
BEAM MAGNETIC RESONANCE TECHNIQUES**

Robert A. Fluegge  
Dr. Dale Headrick  
Dr. Donald Landman

Cornell Aeronautical Laboratory, Inc.

**Approved for public release;  
distribution unlimited.**



## FOREWORD

The research effort reported herein is part of an overall laboratory support program which was formulated by Lt Col R. M. Dowe of ARPA in support of ARPA Project SECEDE. This program is administered by personnel of the Environmental Studies Section at RADC and consists of the following efforts:

**Contractor:** City College of New York

**Principal Investigator:** Professor C. M. Tchen

**Research Area:** Theoretical study of the motion and diffusion of neutral and ionized components of metallic vapor clouds including striation development from instabilities.

**Contractor:** General Electric Space Electronics Lab., Philadelphia

**Principal Investigator:** Dr. M. J. Linevsky

**Research Area:** Experimental determination of oscillator strengths and photoexcitation mechanisms for barium/air processes.

**Contractor:** AVCO Everett Research Labs.

**Principal Investigator:** Dr. B. Kivel

**Research Area:** Correlation of observed radar and optical data for the purpose of developing a kinetic model for the ionization and transport processes involved in high altitude barium releases.

**Contractor:** Cornell Aeronautical Labs., Buffalo, NY

**Principal Investigator:** R. A. Fluegge

**Research Area:** Experimental investigation of the production and photoionization of metastable states of atomic barium.

**Contractor:** Thiokol Chemical Co., Ogden, Utah

**Investigators:** Dr. R. Reed and Dr. R. G. Billings

**Research Area:** Development of improved chemical mixes and release techniques to improve the production of barium vapor in high altitude releases.

## TABLE OF CONTENTS

	Page No.
INTRODUCTION . . . . .	1
I. BARIUM EXPERIMENTS . . . . .	2
A. Metastable Depopulation . . . . .	2
B. Ionization Experiments. . . . .	8
C. Discussion and Conclusions. . . . .	14
II. METAL OXIDE INVESTIGATIONS . . . . .	15
A. Barium Oxide . . . . .	15
B. Product and Reactant Electronic States. . . . .	18
C. Harpoon Model Predictions for the Reactive Cross Sections . . . . .	18
D. Aluminum Oxide. . . . .	21
E. Boron Oxide. . . . .	25
III. REFERENCES. . . . .	27

## INTRODUCTION

Our experimental program has been continued to measure in the laboratory some of the parameters governing the production of ions in barium. The experiments were performed by creating the metastable states ( $^1D_2$ ,  $^3D_3$ ,  $^3D_2$ ,  $^3D_1$ ) by electron bombardment, exposing the atomic beam to an intense light flux at one of several passbands, and analyzing the resultant metastable depopulation using the CAL Molecular Beam Magnetic Resonance Apparatus (MBMRA). Another set of experiments was performed to collect the resultant photoions directly, using several different light passbands.

Our results confirmed our previous observation of depopulation of the metastables by UV light with the concurrent increase in the number of ions. Results further indicate that the responsible bands are 2990 to 3090Å, ionizing either the triplet or singlet metastables, and 3190 to 3270Å, contributing ions from the singlet metastable.

The sections on reactive scattering of the metal oxides concentrate on Ba, Al, and B incident on  $O_2$  molecules. Metastable states in the metals, as well as the  $O_2(^1\Delta_g)$  metastable, have been included to indicate their effects on the reactive scattering cross sections and their probable contributions to internal energy of the metal oxides.

I would like to acknowledge the significant contributions to this work by Dr. Dale Headrick and Dr. Donald Landman, both in the Molecular Physics Section at CAL.

## I. BARIUM EXPERIMENTS

### A. Metastable Depopulation

The principal advantage of the CAL beam apparatus lies in its capability for separating the (paramagnetic) metastable atom resonances in a magnetic field according to their Landé  $g$  values. At a predetermined magnetic field and rf frequency, one obtains an output that is determined by the atomic mass as well as the Landé  $g$  values. An alternate method of operating the apparatus, using the Majorana (zero-field) transition, allows us to achieve a much larger signal by refocusing all paramagnetic states at the same time. The details of operation of our magnetic resonance apparatus are discussed in Appendix A of Ref. 1. Briefly, the A-magnet focuses those atoms in states with  $m_j > 0$  (electron spin opposing the magnetic field) toward the axis of symmetry in the C-region, where an rf signal flips the electron spin over to allow the B-magnet to refocus these atoms into the detector. By the Majorana transitions, one accomplishes a similar effect by sweeping the C-magnet through zero field, where the atoms "forget" which state they are in, and roughly half will appear in the B-region with spin-up and be refocused. Since this type of transition doesn't depend on the  $g_j$  value, all four metastable states in barium are refocused at the same time. Studies on a collision-free beam of barium atoms are reported here. Since the ground state atoms are non-paramagnetic, they are not deflected by the focusing magnets and very few pass through the off-axis entrance port to the quadrupole mass-spectrometer detector. They add only a small contribution to the off-axis background signal.

As detailed in our previous reports, we focus onto the atomic beam the output of a 5000W xenon-mercury arc lamp, yielding a broadband light flux approximately  $10^4$  times that of the sun at the top of the atmosphere. A chemical filter ( $\text{NiSO}_4 + \text{CoSO}_4$ ) is available to limit the spectrum to the UV ( $2300\text{\AA}$  to  $3400\text{\AA}$ ). A series of narrow passband filters has been selected:  $2955 \pm 30\text{\AA}$ ,  $3005 \pm 55\text{\AA}$ ,  $3265 \pm 25\text{\AA}$ , and  $3735 \pm 25\text{\AA}$ ; but due to manufacturer's delay only the  $3005\text{\AA}$  filter was available for the metastable-depopulation

experiments; the others were used in our more recent work as described in the direct ionization measurements. In order to investigate the broad transition around  $3266\text{\AA}$  from the  $^1D_2$  to the lowest autoionizing level, the combination of the chemical filter and a glass microscope slide was used to pass the band  $3090 - 3325\text{\AA}$ . The filter transmission curves from  $2900 - 3300\text{\AA}$  are shown in Figures 1, 2, and 3, where the filters are labeled by their full width at half maximum. The suffixed letter C (e. g. 2955C) refers to the combination of the chemical filter and the  $2955\text{\AA}$  filter.

The analytically expected decrease in the Ba metastable beam intensity (assuming no mechanisms are present that increase these metastable concentrations) is given by

$$\frac{\Delta N_{\text{Tot}}}{N_{\text{Tot}}} = \frac{\pi}{4} \sigma_o I_{\text{Net}} \frac{D}{v} \quad (1)$$

where:  $D$  = diameter of both the intersecting atomic barium beam and the collimated light beam; both intersect each other on axis, in cm.

$N_{\text{Tot}}$  = the total metastable atom flux arriving at the detector per second.

$\Delta N_{\text{Tot}}$  = the total metastable atom flux changes that have occurred in the atomic beam due to photon absorption.

$I_{\text{Net}}$  = light intensity in photons/cm<sup>2</sup> sec at the atomic beam.

$v$  = effective passband velocity through the molecular beams machine; about  $5.4 \times 10^4$  cm/sec.

$\sigma_o$  = photodepopulation cross section out of the metastable states.

The photodepopulation cross section can be related to an effective oscillator strength,  $f$ , by

$$\sigma_o = \frac{\pi e^2 f}{mc \Delta \nu} \quad (2)$$

where:  $e$  =  $4.8 \times 10^{-10}$  esu

$m$  =  $9.11 \times 10^{-28}$  gm

$c$  =  $3 \times 10^{10}$  cm/sec

$\Delta \nu$  = photon bandpass frequency in sec<sup>-1</sup>

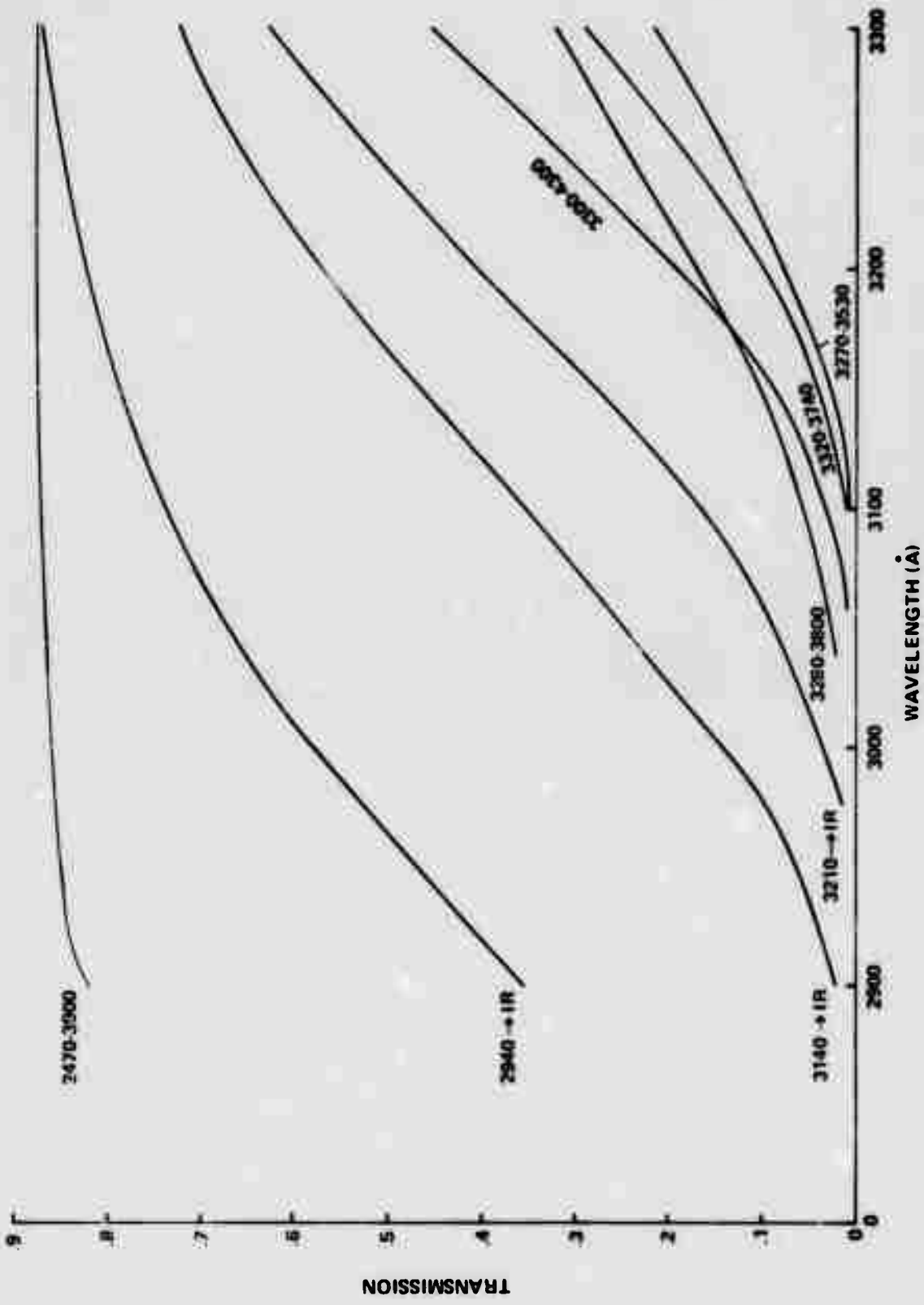


Figure 1 FILTER TRANSMISSION CURVES

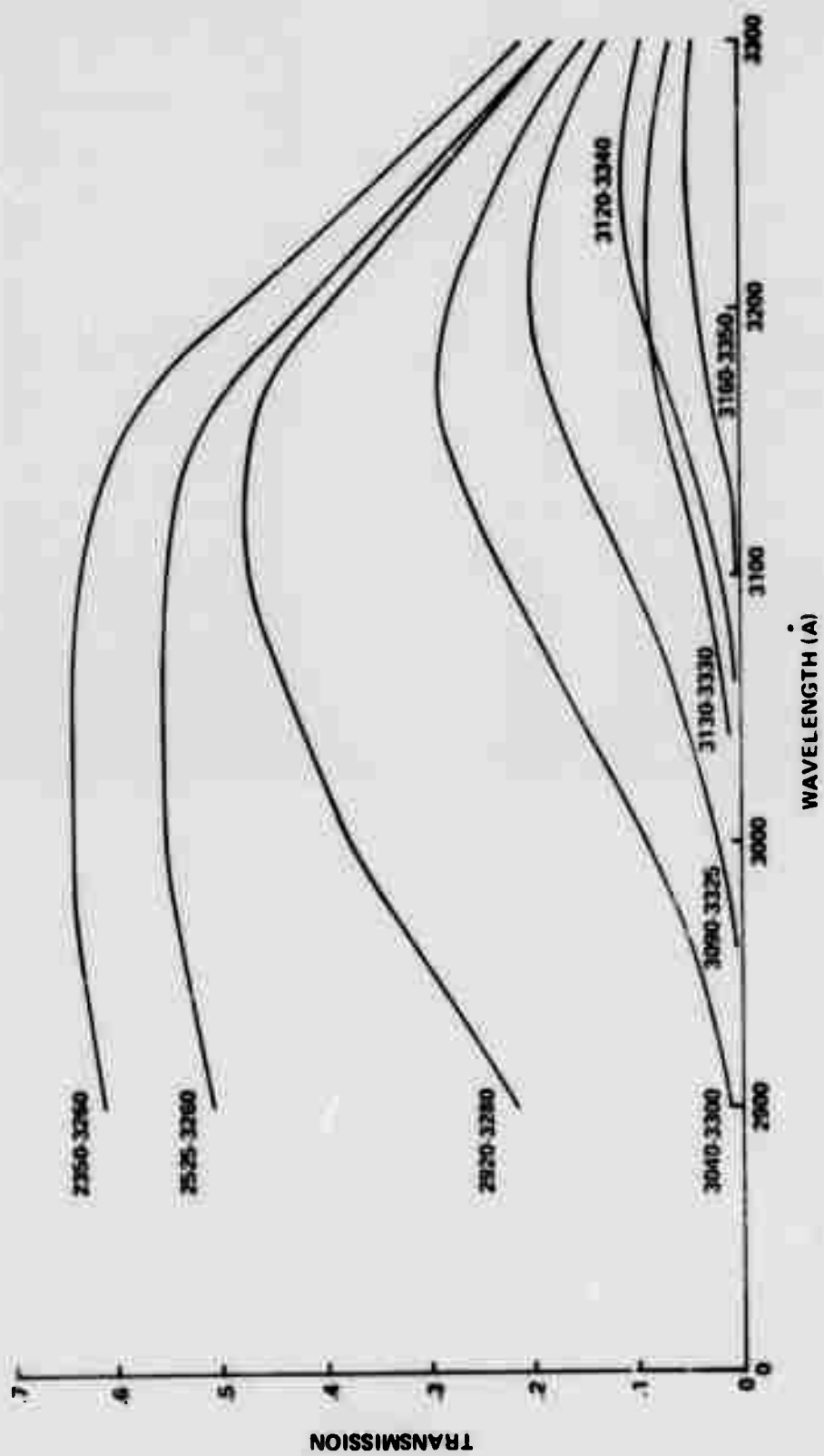


Figure 2 FILTER TRANSMISSION CURVES WITH CHEMICAL FILTER

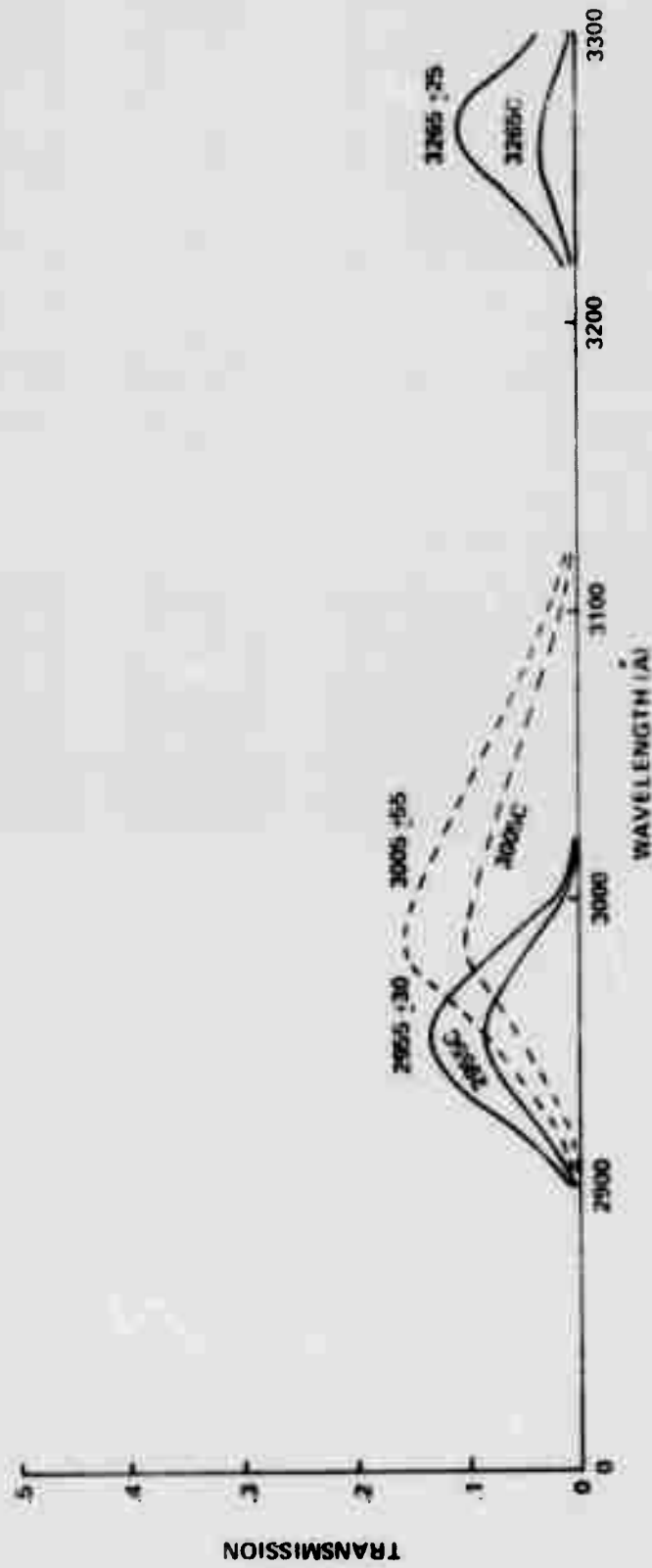


Figure 3 FILTER TRANSMISSION CURVES

By mounting different filters on a chopper wheel and sorting the data into the respective quarters in the multichannel analyzer, we are able to investigate four different passbands simultaneously, with or without the chemical filter, in either the Majorana or the resonance mode. The resonance data were not reproducible; hence, this discussion will only consider the Majorana data. The experimental results for the relative depopulation  $\Delta N/N$  are summarized in Table 1.

Table 1: Passband of Filter Configuration

FILTER	PASSBAND		EXPERIMENTAL $\Delta N/N$
None	UV	IR	-1.6%
Chemical	2350	3260	-1.6
Glass Slide	3210	IR	-0.8
Chemical + glass	3090	3325	0 ± 1
3005Å	3005 ± 55		-3.1
Chemical + 3005Å	3005 ± 55		-2.6

The experimental observations show that:

(1) The  $\Delta N/N$  depopulation when using the chemical filter is the same as from the full spectrum and agrees with our previous results (-1.5% as per our August Report) when the light intensity variations are taken into account. This implies that only the UV region (2350 - 3260Å) is effective for increasing and/or decreasing the metastable populations.

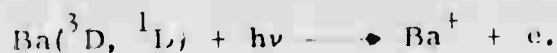
(2) The depopulation due to light passing through the 3005C filter was consistently greater than through the chemical filter (2350-3260Å), even though the latter has a much high transmission (65% as opposed to 10%). This implies that there is some pumping in the UV region outside of the 3005 ± 55Å passband, such as by the 3071Å line from the ground state to the  $7p \ ^1P_1'$  level with decay to the metastable levels.

(3) The 3210  $\rightarrow$  IR bandpass produces less than a 1% decrease in the metastable populations, and the losses due to illumination from the 3090 - 3325 averaged to zero within about a 1% standard deviation. This substantiates that the bulk of the transitions into and out of the barium metastables occurs at wavelengths shorter than 3300Å.

Our best results were obtained using the 3005 filter. This filter passes as many as 11 triplet and 3 singlet lines to one of the several known autoionizing levels. No similar data for the bands near 3200Å were obtained in this series of experiments. However, as will be seen in the next section, decreases in the  $^1D$  metastables do occur at these somewhat longer wavelengths.

#### B. Ionization Experiments

In order to get a more direct indication of photoionization, experiments were performed so as to collect Ba ions directly. Ionization occurs according to



The same oven and metastabilizer as reported in Section A are used to generate the barium beam, and an electron multiplier is installed just beyond the light-interaction region and slightly above the beam axis (see Figure 4). The first dynode of the multiplier is held at -1500V to collect photoions. Both electric and magnetic deflecting fields are used in the oven chamber to prevent ions created by electron bombardment from reaching the multiplier. A cylindrical light shield is used to keep the intense UV light off the first dynode. Without this shield we find that the photoelectron signals dominate; with this light shield an output signal that is only 4% of a comparable beam signal is measured. These small corrections are applied to that data where needed. The neutral barium beam is monitored using a quadrupole mass spectrometer. The simultaneous output of the photoion collecting multiplier is sorted into quarters of our multichannel scaler corresponding to the filter rotated into the light beam. The configuration is similar to that described in A.

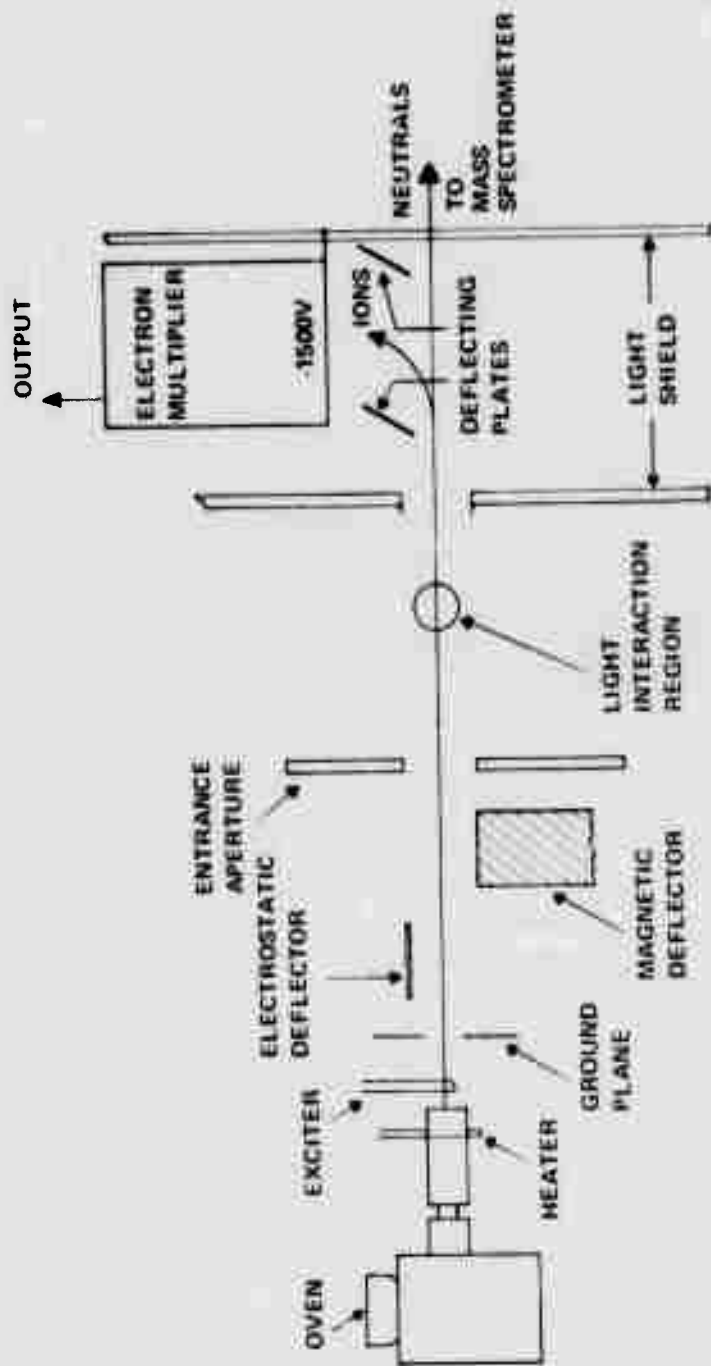


Figure 4 PHOTOION DETECTOR

The relative ionizations found using our 5000 watt Hg-Xe lamp are shown in Figures 5 and 6. The various light-bandpasses used are aligned along the abscissa according to the calculated relative outputs found by assuming that 50% of the ionization occurs due to light in the 2990 - 3090Å band and the other 50% occurs due to light in the 3190 - 3270Å band. The outputs in Figure 5 are recorded relative to the ionization measured in the open (no filter) position. Each series is normalized to full-on and full-off filter positions. For example, the relative ionization for the 2490 - 3900Å band should be 86% of that measured in the full open configuration as estimated using our measured light intensity and filter transmissions. Instead however, we measure between .32 and .48 of the "full-on" values. The reason for this factor of 2 difference is not clear at present, but probably is associated with the non-linear output signals measured in the full-on positions. Nearly every output in this position is seen to increase slowly with time (over the 3 second ion-collection period), although no similar signals are found when using the light filters listed above.

Since the Hg-Xe lamp output contains a series of short, intense lines in the wavelength ranges of primary interest, it was replaced by a 1000 watt xenon arc lamp. Our spectral measurements show that the latter has a much smoother, more uniform output over the complete spectrum. This, in effect, minimized the interpretation problems associated with the resulting photoionization. Summary of the measured positive-ion currents are given in Figures 7, 8, and 9. They are given relative to the on position for three assumptions: (1) Figure 7 presents the light passband on the abscissa position corresponding to its calculated relative light transmission. The solid curve assumes that 50% of the ionization occurs in the 2990 - 3090Å region, and 50% of the ionization occurs in the 3190 - 3270Å region. This results in a reasonably good fit to the data points as shown. (2) Figure 8 has included in the passband locations (on the abscissa) the assumption that all ionization occurs in the 2990 - 3090Å regions, and (3) Figure 9 includes the assumption that all ionization occurs in the 3190 - 3270Å band. The effect of these different assumptions is to relocate the various pass-band positions, and as seen, assumptions 2 and 3 result in a somewhat poorer fit.

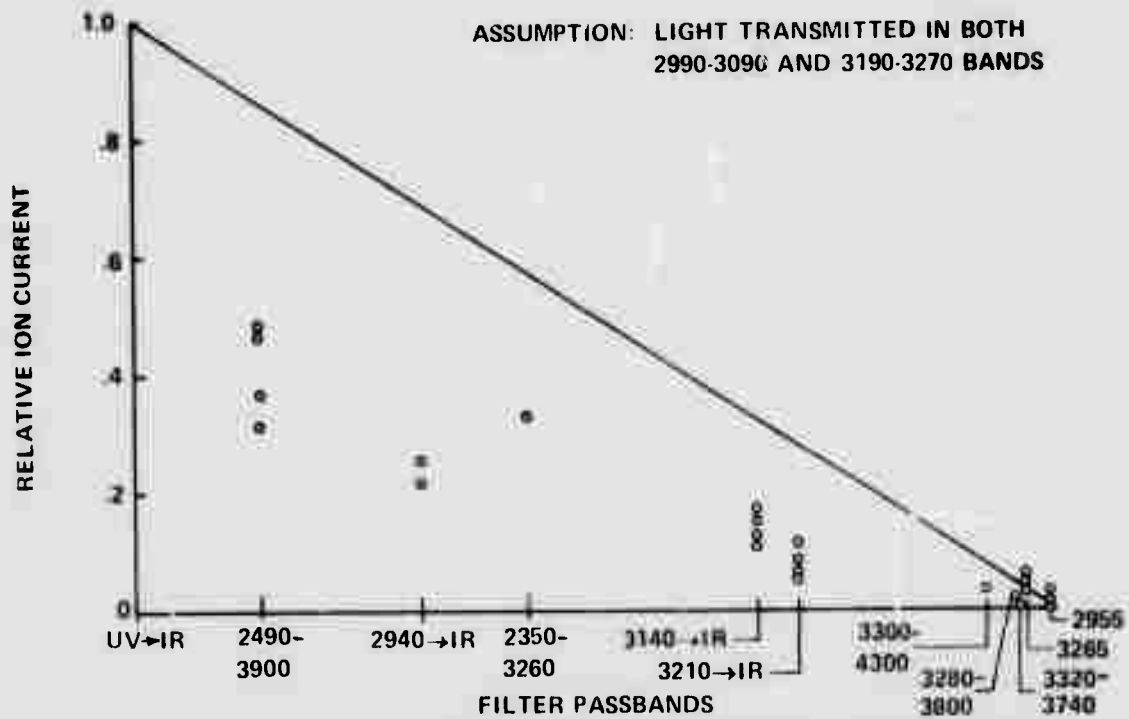


Figure 5 IONIZATION RESULTING FROM ILLUMINATION USING Hg-Xe LAMP

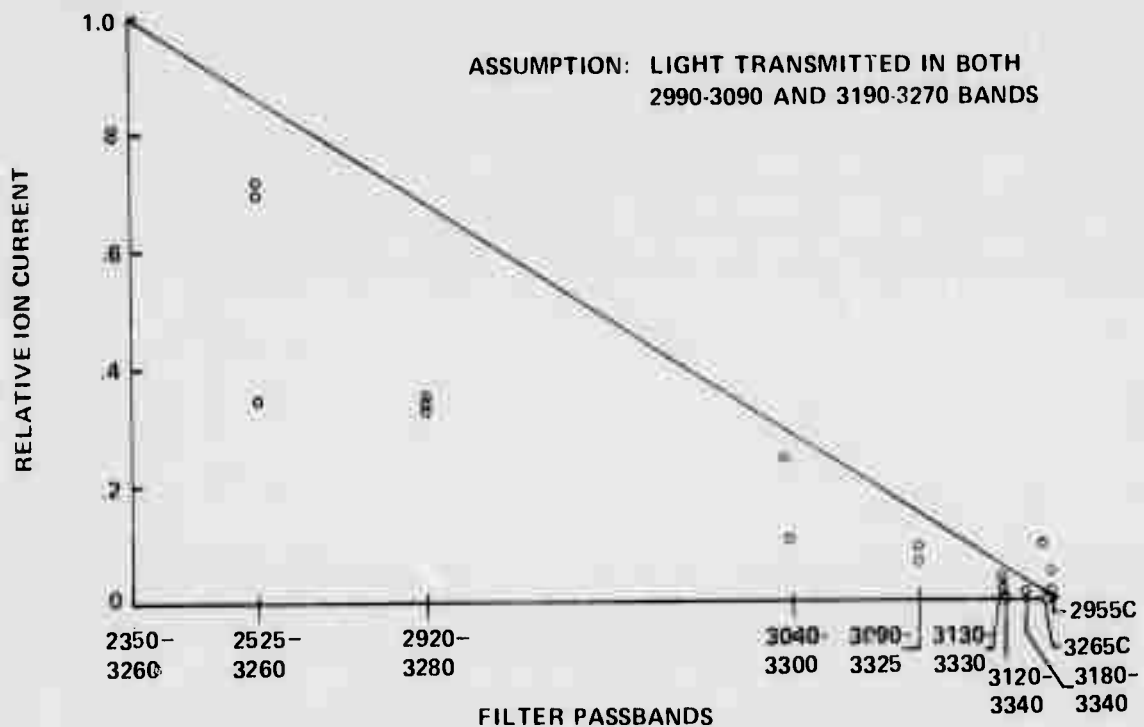


Figure 6 IONIZATION RESULTING FROM ILLUMINATION USING Hg-Xe LAMP AND CHEMICAL FILTER

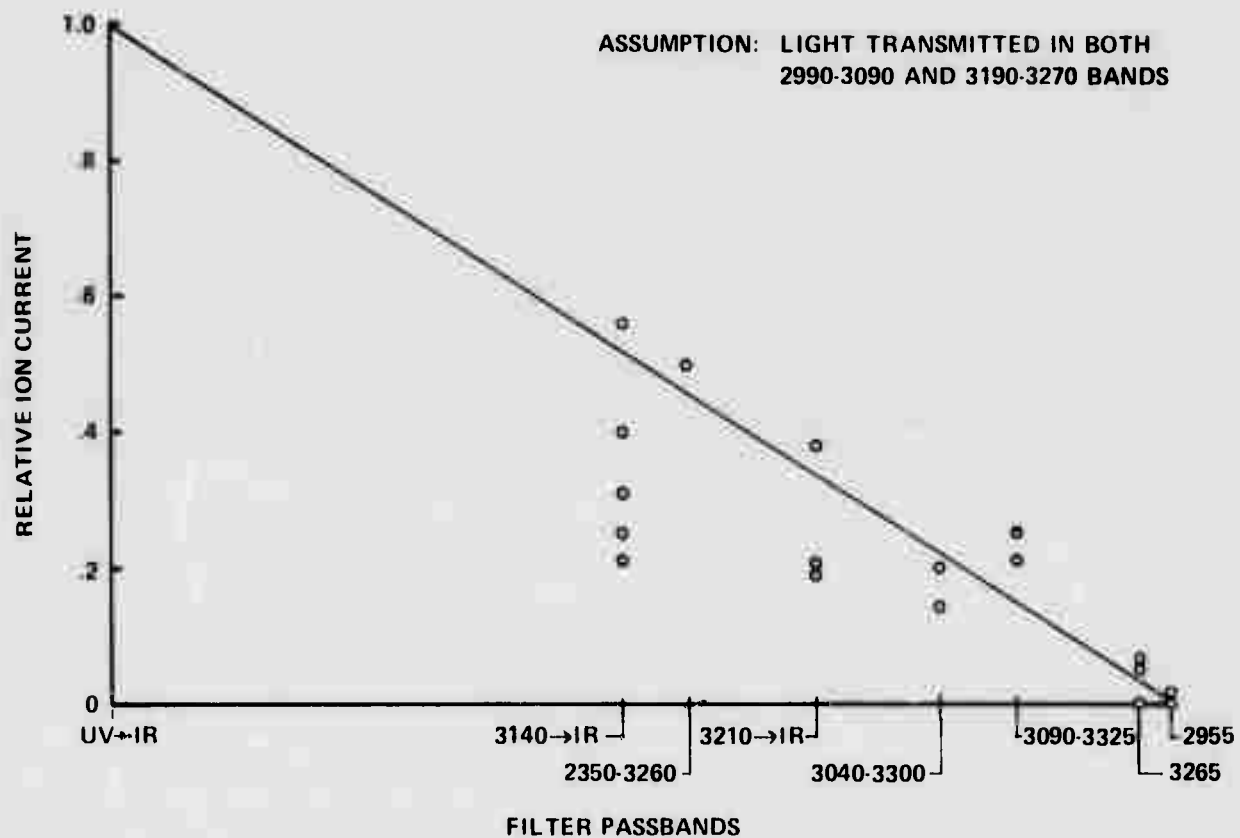


Figure 7 IONIZATION RESULTING FROM ILLUMINATION WITH Xe LAMP

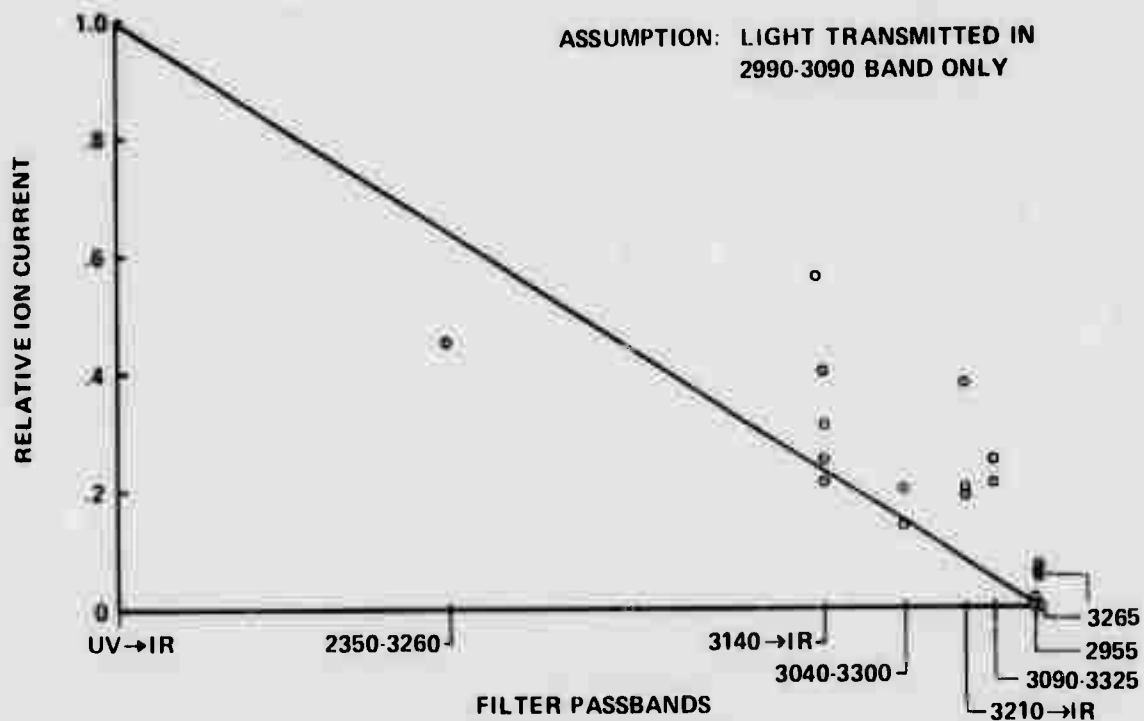


Figure 8 IONIZATION RESULTING FROM ILLUMINATION WITH Xe LAMP

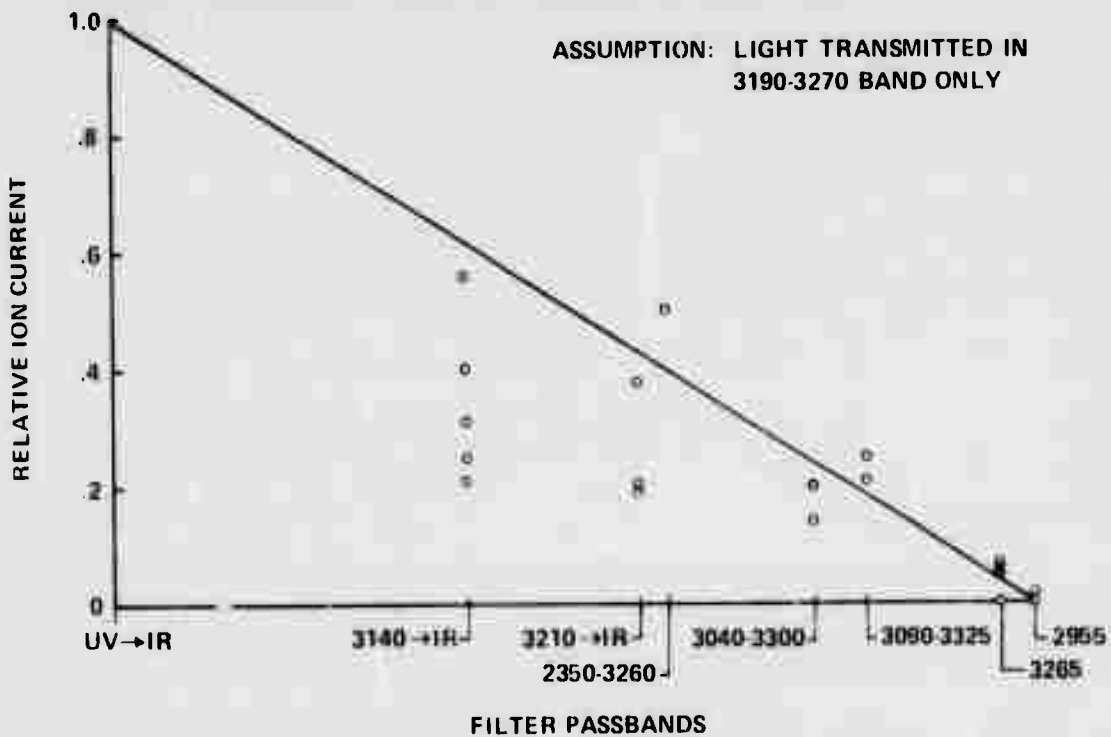


Figure 9 IONIZATION RESULTING FROM ILLUMINATION WITH Xe LAMP

In all cases we find a somewhat greater signal with the 3265Å filter (transmitting only the lines from the  $^1D_2$  metastable) than with the 2955Å filter (transmitting several lines from the  $^3D$  metastables). Since our metastabilizer creates equal populations of the four metastable states, this indicates a strong role for  $^1D_2$  metastables in the ionization process. Furthermore, the data indicate that the bulk of the ionization occurs at wavelengths greater than 3000Å as might be expected for strong auto-ionizing states.

### C. Discussion and Conclusions

Both the depopulation and ionization experiments are consistent and confirm that the metastable states in barium are strong contributors to photoionization in barium clouds under solar radiation. Both the singlet and triplet states contribute. From the depopulation experiments we find that major losses occur due to photons near 3005Å and that considerable metastable density increases occur when the atomic beam is subjected to a full light spectrum. Almost 50% of the atom-loss processes were compensated for by pumping mechanisms that added metastables to the beam. The wavelengths that cause the greatest increases in the metastables lie in the UV regions. Results from the ionization experiments show that roughly half of the photoionization (for equally populated metastables) occurs from the singlets and half from the triplet metastables. These results also show that ionization occurs mainly from photons having wavelengths longer than 3000Å. These results are at variance with the shape of the cross section curves recently reported by Linevsky<sup>2</sup>; he finds strong ionization occurs at wavelengths below 3000Å and almost no ionization at 3250Å. We plan to isolate the responsible wavelengths more precisely and report on them in our next semiannual report.

## II. METAL OXIDE INVESTIGATIONS

Mechanisms that decrease metal atom densities have been analytically investigated during this period; we have concentrated on the loss process:



for barium, aluminum, and boron. Both barium and boron react exothermically with ground state oxygen molecules, but the aluminum reaction is endothermic by about 0.5 electron volts (eV). The increase in reaction cross sections due to metastable states in the reactants have been estimated using the Harpoon model, and these results are presented. We have considered the four metastables in barium ( $^1D_2$ ,  $^3D_1$ ,  $^3D_2$ ,  $^3D_3$ ) about 1.2 eV above the ground state, the Al( $^4P$ ) metastable 3.6 eV above its ground state, the B( $^4P$ ) metastable up 3.6 eV, and the  $\text{O}_2(^1\Delta_g)$  metastable at 1.0 eV.

To facilitate the analysis of these kinds of collisions, we have chosen to discuss them from the point of view of a controlled laboratory experiment rather than the more general situation normally found in the upper atmosphere. Of course these specific results can be applied to the normal situation through judicious extrapolations. The development and use of our metastabilizer in the photodepopulation and ionization studies presented earlier has made it possible to consider measuring in the laboratory these reactive scattering cross sections. We visualize a crossed beam experiment with the reactants intersecting at  $90^\circ$ . Product atoms and molecules will be scattered according to the kinetics and reactivities carried into the collisions. Newton diagrams, energy analyses, effects of metastable electronic states, potential energy curves for the metal oxides, and predicted cross sections have been included.

### A. Barium Oxide

A Newton diagram for the Ba- $\text{O}_2$  system is shown in Figure 10; barium is shown entering at the left and oxygen shown as traveling vertically. Using classical mechanics, we find the expected scattering when the Ba beam is located at  $90^\circ$  with respect to an  $\text{O}_2$  beam as shown:

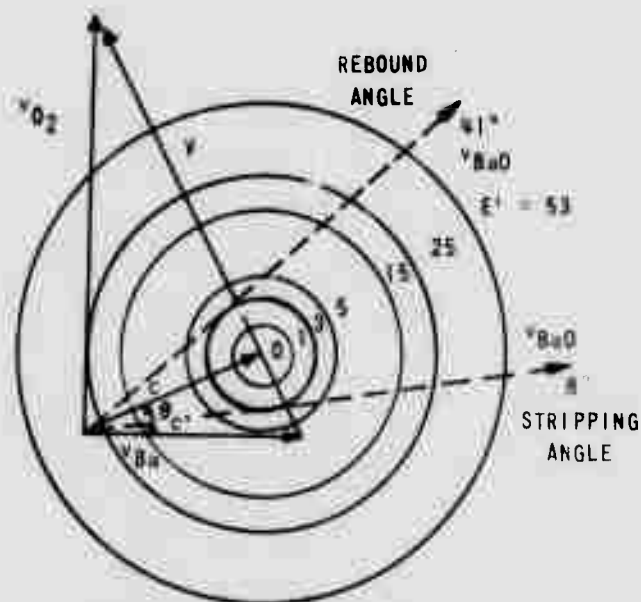


Figure 10 NEWTON DIAGRAM FOR Ba - O<sub>2</sub> SYSTEM

where:  $v_{Ba} = \left( \frac{3kT}{M} \right)^{1/2} \sim 4.6 \times 10^4$  cm/sec for  $T = 1150^\circ K$  (4)

$v_{O_2} \sim 8.8 \times 10^4$  cm/sec for  $T = 1000^\circ K$

$V$  = initial relative velocity

$C$  = center of mass velocity  $\sim 5.4 \times 10^4$  cm/sec

$\theta_c = \tan^{-1} \frac{M_{O_2} v_{O_2}}{M_{Ba} v_{Ba}} = 24^\circ$

The initial relative translational energy,  $E$ , is given by

$$E = 1/2 M_{Ba} v_{Ba}^2 + 1/2 M_{O_2} v_{O_2}^2 - 1/2 M_{Total} C^2 \sim 3.1 \text{ kcal} \quad (5)$$

and the final relative translational energy is:

$$E' = 1/2 \mu (V')^2 \sim 1.73 \times 10^{-10} (V')^2 \text{ kcal} \quad (6)$$

where:  $V'$  = final relative velocity, cm/sec

$\mu$  = the reduced mass

Energy conservation requires that

$$E' + W'_0 + W'_{\text{BaO}} = E + W_{\text{O}_2} + W_{\text{Ba}} + \Delta D^{\circ}_0 \quad (7)$$

where:  $W$  = internal excitation of the various species

$$\Delta D^{\circ}_0 = D^{\circ}_0(\text{BaO}) - D^{\circ}_0(\text{O}_2) = 133 - 117 \text{ kcal} \quad (8)$$

Figure 10 shows a series of circles that correspond to the magnitudes of the recoil velocity vectors for BaO for various values of  $E'$ . The maximum energy available for translational energy in the Ba-O<sub>2</sub> system will occur when the reacting barium is in its metastable <sup>1</sup>D<sub>2</sub> state. The oxygen beam is considered primarily in its ground vibrational state (~9% in its 1st vibrational level), and the O<sub>2</sub> molecule has a most-probable rotational energy at 1 kcal (J=14) at 1000°K. Then:

$$\text{Max } E' = 53 \text{ kcal}$$

where:  $W_{\text{Ba}}$  = 53 kcal for the <sup>1</sup>D<sub>2</sub> state of Ba

$$\Delta D^{\circ}_0 = 16 \text{ kcal}$$

$$E = 3.1 \text{ kcal}$$

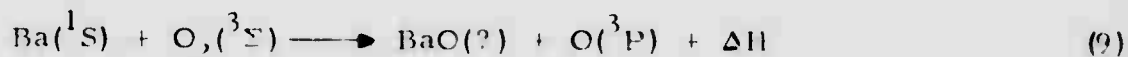
$$W_{\text{O}_2} = 1.0 \text{ kcal}$$

$$W'_{\text{BaO}} = W'_0 = 0$$

However, as evident in similar systems we would expect the final relative translational energy ( $E'$ ) to be nearly equal to the initial relative translational energy ( $E$ ). Thus, under the assumption that  $E = E'$ , the two limits of the laboratory scattering angle (shown by the dashed lines in Figure 10) are estimated. This would put the BaO scattering angle between 8° and 41° in the laboratory coordinate system. The two limits are by chance almost coincident with the rebound angle (41°) and the stripping angle (8°) found by assuming that the BaO recoils along  $V$ .

## B. Product and Reactant Electronic States

Accepted values for the dissociation energies of BaO (133 kcal) and O<sub>2</sub> (118 kcal) show the reaction



where:  $\Delta\text{H}$  = the heat of reaction

to be exothermic by 15 kcal; thus the reaction can proceed on an energy basis even for ground state atoms. Most experimental evidence indicates that the ground state configuration of BaO is  $^1\Sigma$ , which cannot be formed from the ground state configurations of Ba( $^1\text{S}_0$ ) and O( $^3\text{P}$ ). Reaction (9) with BaO( $^1\Sigma$ ) is allowed, however, as long as the emitted O atoms are in a triplet state. Some authors have postulated  $^3\Sigma$  or  $^3\Pi$  states for the BaO molecule; to emphasize this situation we have put together our best guess as to potential energy curves for BaO as given in Figure 11. The ground state combination Ba( $^1\text{S}$ ) + O( $^3\text{P}$ ) remains a question. We show a Morse potential fit to the basic parameters as listed by Herzberg<sup>3</sup> along with a coulomb interaction curve for both the Ba<sup>+</sup>-O<sub>2</sub><sup>-</sup> and Ba<sup>+</sup>-O<sup>-</sup> systems. If the barium reaction can be shown to be ionic in nature, the prohibited crossing rules could be effective here and distort the potential energy curves considerably.

Reactions of the barium metastables with O<sub>2</sub> result in about 53 kcal of energy available to the reaction as pointed out above. Most of this is expected to end up as vibrational or electronic energy of either the BaO or O products. BaO has an excited A $^1\Sigma$  electronic state about 48 kcal above its X $^1\Sigma$  ground state, and O( $^1\text{D}$ ), with an internal excitation near 45 kcal, is the lowest excited electronic state available to the O atom. Vibrational excitation in BaO is probable and could take up a fair portion of the exothermic reaction energy, while a much smaller portion could end up as increased translational energy.

## C. Harpoon Model Predictions for the Reactive Cross Sections

When applied to the Ba-O<sub>2</sub> system, the Harpoon model as outlined by Herschbach<sup>4</sup> predicts that the reactive scattering cross section for the

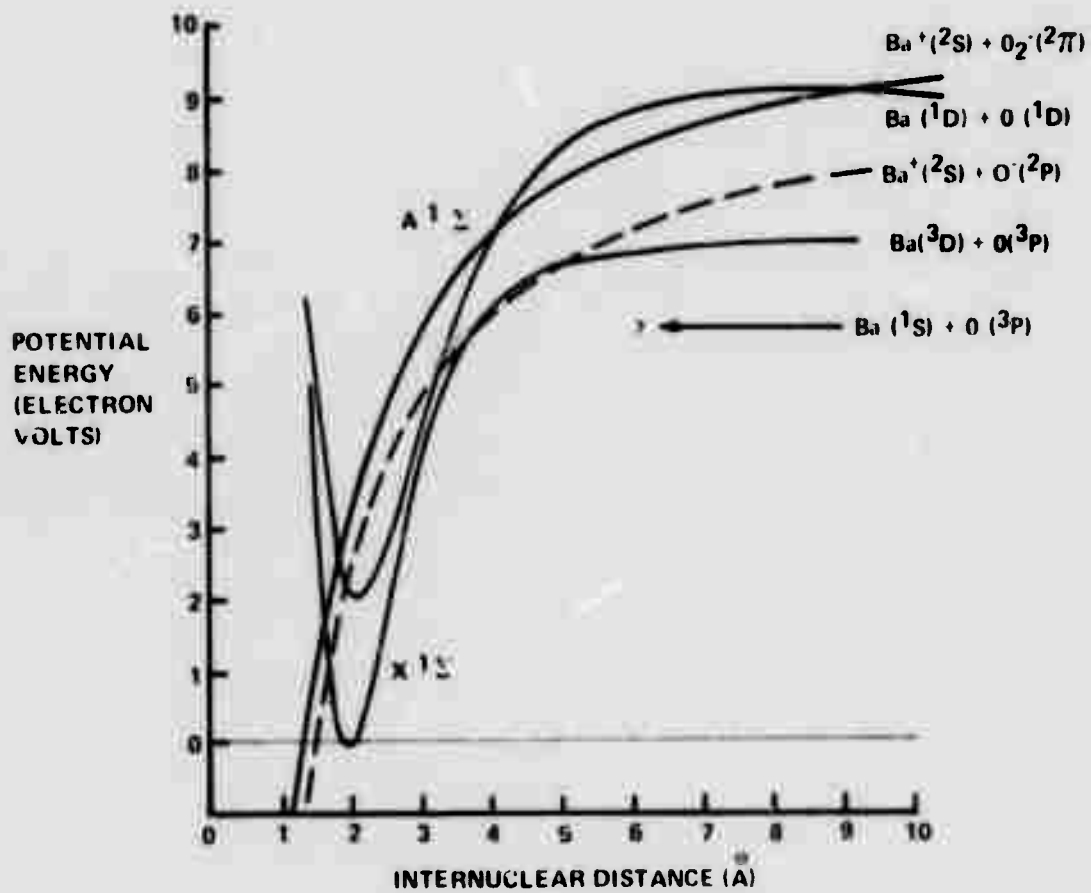


Figure 11 ESTIMATED POTENTIAL ENERGY CURVES FOR BaO

Ba metastables would be almost twice as large as for ground state atoms. The difference is due to the lower ionization potential for the metastables and, hence, a looser bond with the jumping electron that forms  $O_2^-$ . The reactions considered as important are:

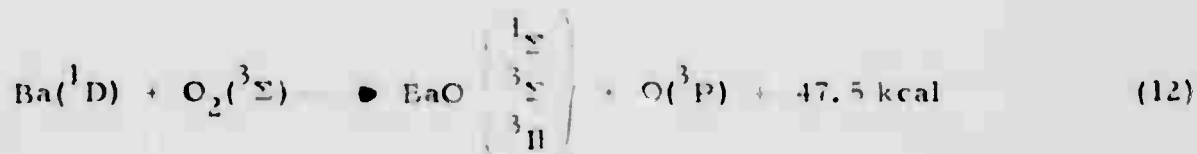
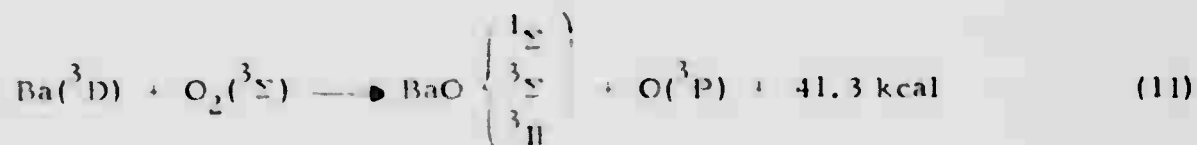
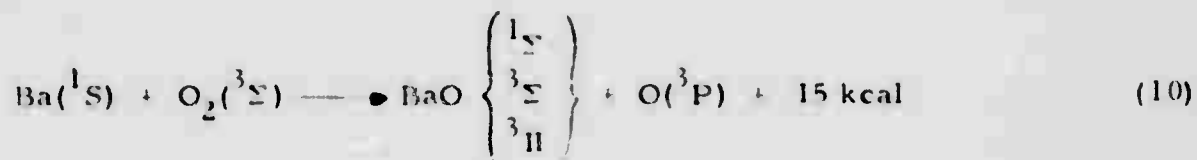


Figure 12 is a potential energy curve for  $O_2$  and  $O_2^-$  as given by Gilmore<sup>5</sup>.

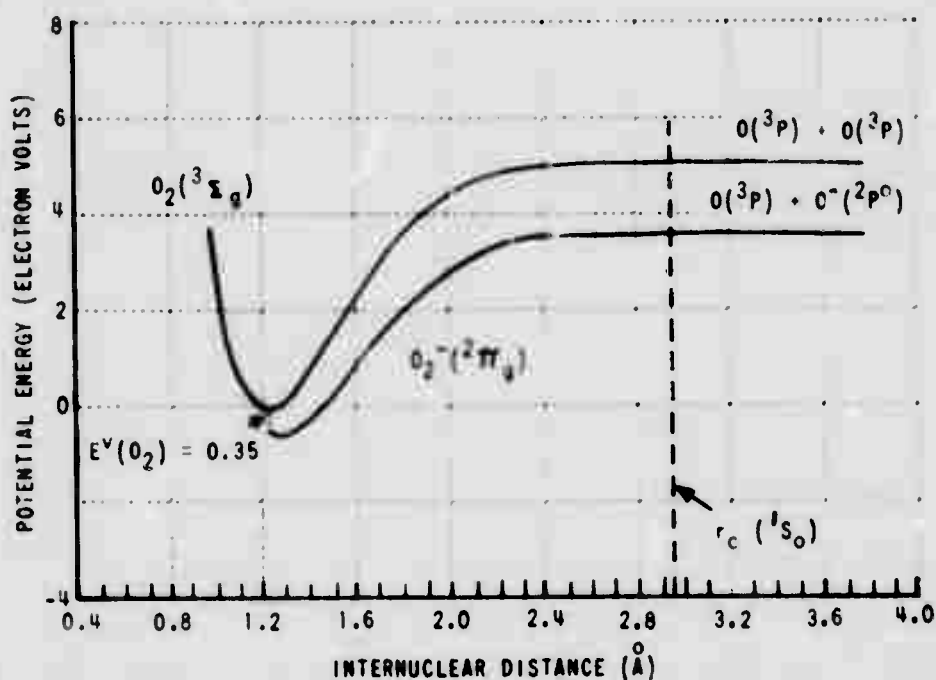


Figure 12 POTENTIAL-ENERGY CURVES FOR  $O_2$  AND  $O_2^-$

At times prior to the Ba-O<sub>2</sub> collision, the O<sub>2</sub> molecule is unaware that Ba is approaching; at a separation r<sub>c</sub>, the electron-jump radius, a vertical transition occurs from the O<sub>2</sub> to the O<sub>2</sub><sup>-</sup> curve, forming an attractive Ba<sup>+</sup> and O<sub>2</sub><sup>-</sup> interaction. The radius at which this occurs is given by

$$r_c = e^2 [I(\text{Ba}) - E^V(\text{O}_2)]^{-1} \approx 2.95 \text{ \AA} \quad (13)$$

where: I(Ba) = 5.210 eV for ground state atoms

$$E^V(\text{O}_2) = 0.35 \text{ eV}$$

The BaO molecule has a high degree of ionic bonding and an equilibrium bond length of 1.94 Å.<sup>3</sup> According to the Harpoon model the total reaction cross section, σ<sub>r</sub>, is approximately

$$\sigma_r = \pi r_c^2 = 27 \text{ \AA}^2 \quad (14)$$

Such relatively small values of σ<sub>r</sub> correlate with rebound scattering and hence we would look for BaO at laboratory angles approaching 41°.

The increased energy of the Ba metastable has a dramatic effect on the ionization potential, I(Ba), in equation (13). The resulting nominal electron jump radii are:

$$r_c(^3\text{D}) \sim 3.9 \text{ \AA}$$

$$r_c(^1\text{D}) \sim 4.2 \text{ \AA}$$

with corresponding total reaction cross sections of

$$\sigma_r(^3\text{D}) \sim 47 \text{ \AA}^2$$

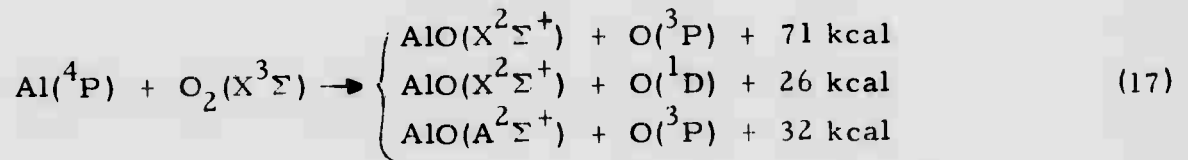
$$\sigma_r(^1\text{D}) \sim 54 \text{ \AA}^2$$

These larger cross sections would be somewhere in between the rebound and stripping limits as evidenced by similar experiments on other systems.

#### D. Aluminum Oxide

The ground state aluminum-O<sub>2</sub> reaction is endothermic by 12 kcal for

ground state  $O_2$ , but 11 kcal exothermic for reactions with the  $O_2(^1\Delta_g)$  metastable. Reactions we consider as likely contributors to losses of aluminum-atom clouds in the upper atmosphere are:



The most-energetically allowed reactions which occur with the  $Al(^4P)$  metastable have sufficient energy to put the  $AlO(X^2\Sigma^+)$  molecule in its 34th vibrational level; thus one could predict considerable emission as the molecule relaxes stepwise to its ground vibrational state.

A Newton diagram for the  $Al-O_2$  system is given in Figure 13. The scattered  $AlO$  should peak someplace between  $11^\circ$  and  $75^\circ$  assuming the final relative translational energy equals the initial value.  $O$  atom scattering will peak under similar assumptions between  $-8^\circ$  and  $111^\circ$ , as shown by the dashed lines in the figure:

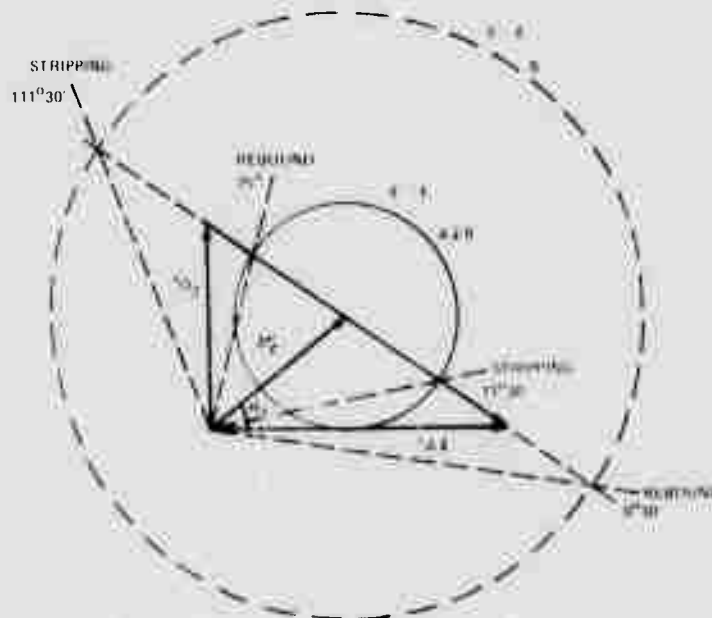


Figure 13 NEWTON DIAGRAM FOR  $Al-O_2$  SYSTEM

where:  $v_{Al} = \left(\frac{3kT}{M}\right)^{1/2} \sim 1.3 \times 10^5 \text{ cm/sec for } T = 1825^\circ\text{K}$

$v_{O_2} \sim 8.8 \times 10^4 \text{ cm/sec for } T = 1000^\circ\text{K}$

$V = \text{initial relative velocity}$

$$\sigma_c = \tan^{-1} \frac{m_{O_2} v_{O_2}}{M_{Al} v_{Al}} = 38^\circ 44'$$

The velocity vector limits indicated in the figure result from energy conservation and the assumption

$$E - E' = W'_{AlO} + W'_O - W_{Al} - W_{O_2} - \Delta D^0_o = 0 \quad (18)$$

where:  $W_X = \text{internal excitation of species } X$

$$\Delta D^0_o = D^0_o(AlO) - D^0_o(O_2) = -12 \text{ kcal.} \quad (19)$$

Thus the reaction of ground state  $(3s^2 3p)^2 P$  Al with ground state  $X^3 \Sigma^-_g$  oxygen is endothermic for the most probable reactant energies,  $E$ . There is some controversy as to the dissociation energy of AlO, but we have chosen to use the 4.6 eV value for these estimates. By considering only the high energy tail of an assumed Boltzman distribution plus estimating that 9% of the  $O_2$  beam is in its first vibrational level at  $1000^\circ\text{K}$ , one can estimate that roughly 8% of the Al- $O_2$  collision will have sufficient energy to proceed. However, such a reaction will involve considerable transfer of translational energy into internal energy.

The  $(3s 3p^2)^4 P$  term of Al is metastable with an excitation energy of 83 kcal. This additional energy permits an additional number of reactions with ground state  $O_2$  to occur as listed in equation 17. Metastable  $O_2(^1 \Delta_g)$  can also add sufficient energy to cause the reaction to proceed on an energy basis as listed in Equation (16).

Our best guess as to potential energy curves for the AlO system is presented in Figure 14. Recent investigations have reopened the uncertainty of the dissociation energy for AlO and produced evidence for at least one

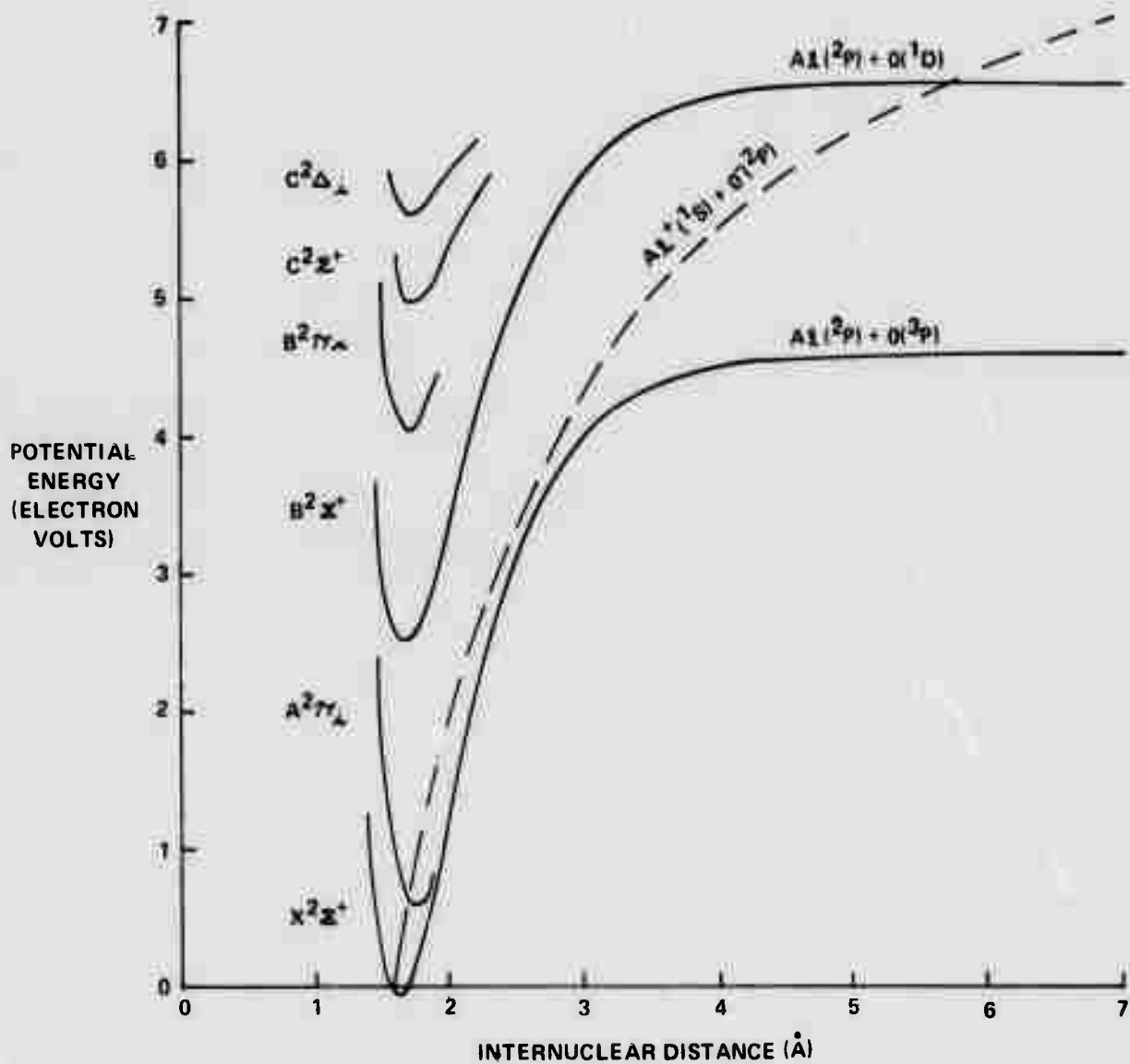


Figure 14 ESTIMATED POTENTIAL-ENERGY CURVES FOR AlO

additional state near the  $\text{AlO}(^2\Sigma^+)$  ground state. McDonald and Innes<sup>6</sup> have found evidence for an  $\text{A}^2\Pi_1$  state 0.655 eV above the ground state. They argue that since both the  $\text{A}^2\Pi_1$  and  $\text{X}^2\Sigma^+$  states give 4.5 eV from Birge-Sponer extrapolations and since the  $\text{X}^2\Sigma^+$  state is likely to be ionic, the dissociation limit must be  $0.655 + 4.5 = 5.2$  eV. The evidence for an ionic ground state is supported by Knight et al.<sup>7</sup>; they find the odd electron being about 82% on the oxygen atom. Thus one would expect that a Birge-Sponer extrapolation for the  $\text{X}^2\Sigma^+$  state would not be valid, but might be valid for the  $\text{A}^2\Pi_1$  state. Again the  $\text{O}_0(^2\text{P}) + \text{Al}^+(^1\text{S})$  coulomb attraction curve has been included to indicate possible distortions to these assumed Morse potential curves. The curves would at least be distorted in the areas near curve crossings.

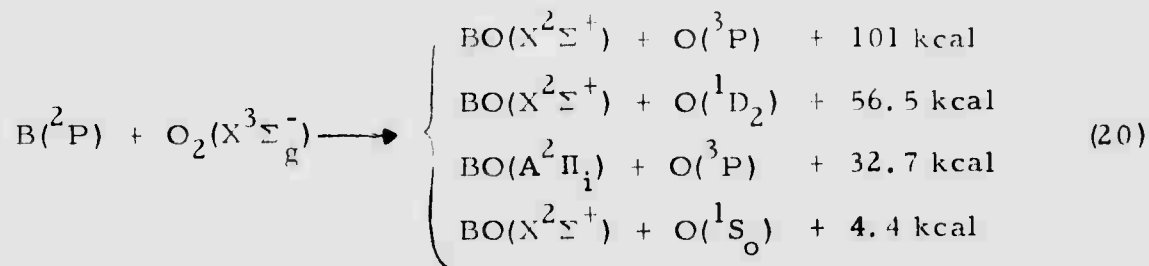
The Harpoon model predictions put the electron jump radii and the reactive cross sections for each of the reactants at:

<u>Reactants</u>	<u>Electron Jump Radius</u>	<u>Cross Section</u>
$\text{Al}(^2\text{P}) + \text{O}_2(^3\Sigma_g^-)$	2.5 Å	20 Å <sup>2</sup>
$\text{Al}(^2\text{P}) + \text{O}_2(^1\Delta_g)$	3.1 Å	30 Å <sup>2</sup>
$\text{Al}(^4\text{P}) + \text{O}_2(^3\Sigma_g^-)$	7.1 Å	158 Å <sup>2</sup>

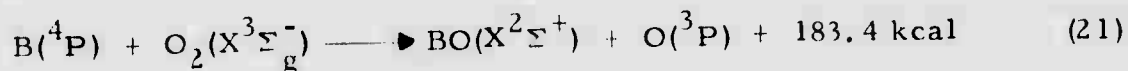
Thus, using the guidelines of Herschbach, the two upper reactions should occur near the rebound scattering angle for  $\text{AlO}$  ( $75^\circ$ ) and the reaction with  $\text{Al}(^4\text{P})$  should most likely occur at the  $11^\circ$  stripping angle.

#### E. Boron Oxide

The boron oxide system is highly exothermic. The ground state reactions energetically possible are:



Boron also has a metastable  $(2s2p^2) ^4P$  term with an excitation energy of 82.4 kcal. Thus in addition to the above reaction products, the possibility exists for



The Harpoon model predicts the following:

<u>Reactant</u>	<u>Electron Jump Radius</u>	<u>Cross Section</u>
$B(^2P) + O_2(^3\Sigma)$	1.8 Å	10 Å <sup>2</sup>
$B(^4P) + O_2(^3\Sigma)$	3.3 Å	34 Å <sup>2</sup>

Thus, especially for the ground state boron reaction, we would expect to find a rebound type reactive scattering.

### III. REFERENCES

1. R. A. Fluegge, "Project Secede, Investigation of Ba Metastables", Semiannual Technical Report No. 1, RADC-TR-69-86, Cornell Aeronautical Laboratory, Inc., January 1969.
2. M. J. Jinevsky, "Study of Optical Energy Transfer Processes", Final Report, RADC-TR-69-291, General Electric Co., July 1969.
3. G. Herzberg, "Spectra of Diatomic Molecules," D. Van Nostrand Co., Inc., New York (1950).
4. D. R. Herschbach, "Reactive Scattering in Molecular Beams," in Advances in Chemical Physics X, J. Ross, Ed., Interscience Publishers, New York (1966).
5. F. R. Gilmore, "Basic Energy Level and Equilibrium Data," in DASA Reaction Rate Handbook, October 1967.
6. J. K. McDonald and K. K. Innes, J. Mol. Spectrosc. 32, 501-510 (1969).
7. L. B. Knight, Jr., W. C. Easley, and W. Weltner, Jr., J. Chem. Phys. 52, 1607 (1970).